NJC

ROYAL SOCIETY OF CHEMISTRY

PAPER

View Article Online
View Journal | View Issue

Cite this: *New J. Chem.*, 2021, **45**, 4746

Palladium nanoparticles *in situ* synthesized on *Cyclea barbata* pectin as a heterogeneous catalyst for Heck coupling in water, the reduction of nitrophenols and alkynes†

Van-Dung Le,‡[ab] T. Cam-Huong Le,‡[ab] Van-Trung Chau,[b] T. Ngoc-Duyen Le,[b] Chi-Hien Dang,*[ab] T. To-Nguyen Vo,[b] Trinh Duy Nguyen [c] and Thanh-Danh Nguyen *[ab]

Received 13th October 2020,
Accepted 10th February 2021

DOI: 10.1039/d0nj05032f

rsc.li/njc

This study develops an effective method for the *in situ* synthesis of palladium nanoparticles (PdNPs) using *Cyclea barbata* pectin as a green reducing and stabilizing reagent. The PdNP@pectin nanocomposite was well characterized by analysis techniques such as UV-vis, FTIR, EDX, XRD, SEM, HR-TEM and STEM-mapping. Crystalline PdNPs were found to be distributed in the size range of 1–25 nm with the highest frequency of 6–12 nm. PdNP@pectin exhibited excellent recyclable catalysis activity for the Heck coupling reaction in water medium. The kinetics and recyclability of nanoparticles were investigated for the catalytic reduction of *o*-, *m*- and *p*-nitrophenol. The result showed a good catalysis efficiency with five successful recycles without compromising much. In particular, the nanocomposite was used as a catalyst for the conversion of alkynes into *cis*-alkenes with KOH/DMF as a hydrogenation source. The reaction was also utilized effectively for the synthesis of sex pheromones, including *Plutella xylostella* ((*Z*)-11-hexadecen-1-yl acetate) and *Cylas formicarius* ((*Z*)-3-dodecen-1-yl(*E*)-2-butenoate) with the total yields of 70% and 68%, respectively. Therefore, PdNPs supported on *C. barbata* pectin are promising catalysis materials for application in various fields.

1. Introduction

Transition metal nanoparticles have been extensively explored for advanced catalysis applications in numerous organic reactions. These nanomaterials play a crucial role in the field of heterogeneous catalysis because their high surface area endows them with many highly active uncoordinated metal sites.[1–3] Recently, PdNPs have attracted tremendous efforts in the study of catalysis due to their broad applications in the pharmaceutical industry, agriculture, biochemistry and environment.[4–8] Green synthesis of PdNPs using organic materials such as plant extracts, natural compounds and polysaccharides possesses many advantages, including effective cost, simple technique and high biocompatibility.[9,10]

Palladium-catalyzed coupling reactions play a vital role in organic synthesis for the assembly of organic molecules with complex structures which are obtained *via* carbon–carbon formation.[11–15] Cross-coupling reactions such as the Heck reaction have been developed using palladium as a homogeneous catalyst. Recently, PdNPs have been explored widely to enhance the catalytic activity and selectivity of these reactions.[16–19] The importance of nanomaterials not only includes the enhancement of synthetic performance, but also promotes the use of mild and less harmful conditions and the development of green chemistry. In fact, PdNP catalysts may enhance cross-coupling reactions in aqueous media without using any ligand or co-catalyst.[20–23]

Hydrogenation of nitrophenols into aminophenols is an important reaction not only in the degradation of toxic compounds but also in the pharmaceutical industry as essential precursors for the synthesis of common drugs, such as paracetamol and phenacetin.[24] Moreover, selective reduction of alkynes into *cis*/*trans*-alkenes has been paid considerable attention in the synthesis of bioactive compounds.[25–27] Hydrogen gas is an effective reducing source that is commonly selected for the hydrogenation of these compounds.[28,29] However, difficulties in the reaction design and production cost, such as special equipment and storage of hydrogen gas, are main problems inducing disadvantages and barriers

[a] *Graduate University of Science and Technology, Vietnam Academy of Science and Technology, 18 Hoang Quoc Viet, Cau Giay, Hanoi, Vietnam. E-mail: dangchihien@gmail.com, danh5463bd@yahoo.com, ntdanh@ict.vast.vn*
[b] *Institute of Chemical Technology, Vietnam Academy of Science and Technology, 1A, TL29 Street, Thanh Loc Ward, District 12, Ho Chi Minh City, Vietnam*
[c] *Center of Excellence for Green Energy and Environmental Nanomaterials, Nguyen Tat Thanh University, Ho Chi Minh City 755414, Vietnam*

† Electronic supplementary information (ESI) available. See DOI: 10.1039/d0nj05032f

‡ These authors contributed equally to this study.

for the application of these reactions in industry. Transfer hydrogenation, which is well known as the addition of hydrogen to a hydrogen-accepting molecule from a source other than H_2, is an important alternative for the synthesis of these derivatives.[30] This method uses various hydrogen-donation sources, including hydrazine,[31] HCOOH,[32] H_2O,[33] $NaBH_4$[34] and DMF.[35]

Cyclea barbata is a species of flowering plant. Its leaves are usually used as a medicinal plant and are also used to produce a jelly that is typically consumed as a stomach medicine.[36] *Cyclea barbata* is distributed widely and used popularly in many countries in Asia, including China, India, Indonesia, Malaysia, Thailand and Vietnam. Its gel has attracted significant attention because it can form at room temperature without any other reagents. The aqueous extract contains pectin chains with a main component of polygalacturonic acid and divalent cations, which can form cross-links during gelation.[37] Application of this pectin has been limited to the food industry to date. Therefore, further application of this pectin should be extended to other fields, such as the environment, energy and catalysis. To the best of our knowledge, the application of this pectin for synthesis of metallic nanoparticles, including PdNPs, has not yet been reported in the literature.

Insect pheromones are chemicals capable of acting like hormones outside of the insect's body. Highly selective synthesis of *cis*/*trans*-alkenes is a particularly important key in the preparation of pheromones of various insect species. In the present work, PdNPs have been synthesized *in situ* using pectin prepared from *Cyclea barbata* leaves as a reductant and stabilizing agent. Their catalytic activity was evaluated for Sonogashira coupling, reduction of nitrophenols and selective hydrogenation of alkynes into *cis*-alkenes as well as its application for synthesis of *Plutella xylostella* and *Cylas formicarius* pheromones.

2. Results and discussion

2.1. Preparation of PdNPs@pectin

The CB pectin was prepared according to a previous report.[38] The main component of CB pectin is well known to be polygalacturonic acid,[39,40] which can transform *in situ* metallic ions into MNPs as reducing and capping agents in aqueous solutions. Pd^{2+} ions were added to the aqueous solution of the pectin and *in situ* reduced under heating at 100 °C to form the composite PdNPs@pectin (Fig. 1). The formation of PdNPs can be observed from the UV-vis spectra (Fig. S1, ESI†). There is no absorption peak in the spectrum of the CB pectin, while the gel solution of Pd^{2+}@pectin possesses a peak at 375 nm ascribed to the charge-transfer transition of Pd^{2+} ions. This peak disappeared after heating at 100 °C for 1 h, which confirms the formation of PdNPs on the CB pectin. The nanocomposite was physicochemically characterized by analysis techniques. The nanocomposite was used as a catalyst for the Heck reaction in water medium, reduction of nitrophenols and reduction of alkynes into *cis*-alkenes; also, its applications in the synthesis of insect pheromones were explored.

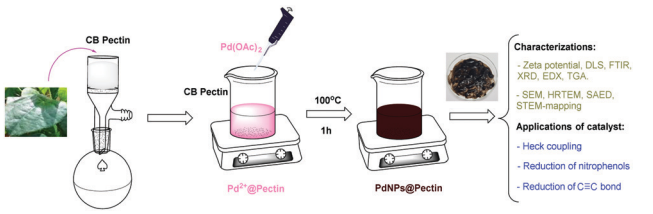

Fig. 1 Schematic of the *in situ* preparation and catalysis application of PdNPs on pectin extracted from *Cyclea barbata* leaves.

2.2. Physicochemical characterization of the catalyst

To study the stabilization of the nanocomposite, solutions of PdNPs@pectin were utilized to investigate the zeta potential and dynamic light scattering (DLS) distribution at 25 °C (Fig. 2A and B). The results showed that the colloidal solution of the synthesized nanocomposite possesses a high negative zeta potential value (−24 mV), which confirms its high stability in aqueous solution. The size distribution profile showed a monodispersed distribution of the nanocomposite PdNPs@pectin in the range of 315–580 nm with a mean hydrodynamic diameter of 455 nm. The results revealed that the synthesized PdNPs were well stabilized by the polymer chains of CB pectin in aqueous solution.

The functional groups of the organic components could be determined by using FTIR measurements. The spectra of CB pectin and the nanocomposite are shown in Fig. 2C. Similar absorption bands are observed from both spectra. For the CB pectin, the broad band recognized at 3408 cm^{-1} is assigned to the OH groups of saccharide. The shoulder that appeared at 1750 cm^{-1} is assigned to the C=O stretching vibration of methyl esterified carboxylic groups, and the sharp peaks at 1639 and 1415 cm^{-1} correspond respectively to symmetric and asymmetric stretching vibrations of COO^- groups of the galacturonic acid units.[41,42] Similar peaks shifted by several wavelength numbers were observed in the spectrum of PdNPs@pectin, which confirmed that the polysaccharide chains played a principal role as stabilization agents of the PdNPs.

The crystalline structure of the PdNPs was determined by X-ray crystallography. Fig. 2D confirms the presence of PdNP crystals in the nanocomposite. The XRD pattern showed peaks with Bragg angle values (2θ) of 40.1°, 46.3° and 68.8°, indexed respectively to reflections from the (111), (200) and (220) planes of the face centred cubic (fcc) crystal structure of metallic palladium.[43,44] The preferential orientation of palladium crystals with strong intensity of the peak at the (111) plane was clearly observed.

The elemental composition presented in the powder composite and average percentages of the elements was determined by EDX measurements (Fig. 2E). The presence of carbon and oxygen confirmed that the organic components appeared in the nanocomposite PdNPs@pectin. The content of elemental palladium found in the powder sample was about 30.7%. Some other elements, including sodium (2.8%) and calcium (3.8%), were also determined.

The thermal behavior of CB pectin and PdNPs@pectin was evaluated by TGA measurements in an air flow of 20 mL min^{-1} at a heating rate of 10 °C min^{-1} (Fig. 2F). Similar thermal

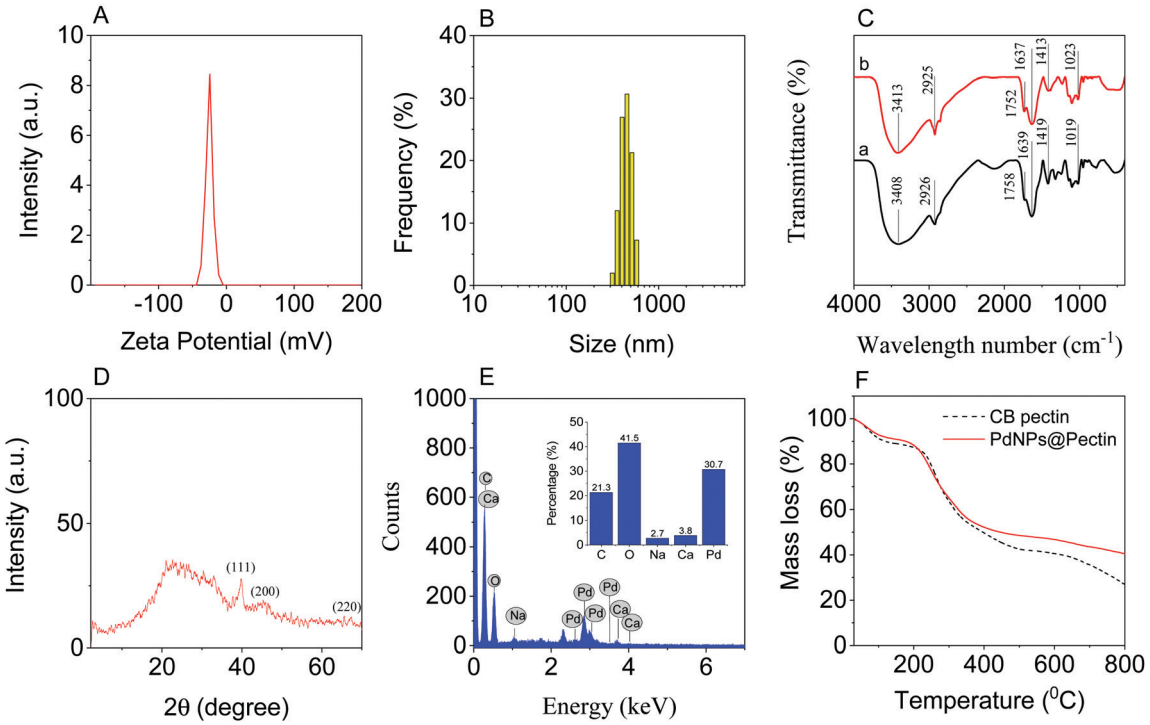

Fig. 2 Zeta potential (A) of PdNPs@pectin; dynamic light scattering (B) of PdNPs@pectin; FT-IR spectra (C) of CB pectin (a) and PdNPs@pectin (b); XRD pattern of PdNPs@pectin (D), EDX spectrum of PdNPs@pectin (E), and TGA curves (F) of CB pectin and PdNPs@pectin in an air flow of 20 mL min^{-1} at a heating rate of 10 °C min^{-1}.

behaviors were observed for both the samples, which occurred in two stages. In the first stage (30–217 °C), the CB pectin and the nanocomposite showed weight losses of 10% and 12%, respectively, which are related to the loss of volatile components and adsorbed water.[45] The weight loss of the nanocomposite was much lower than that of CB pectin in the next temperature range of 217–800 °C. The weight loss of CB pectin is about 61%, while that of PdNPs@pectin is about 49%. Thus, the ash of the nanocomposite (41%) is much higher than that of CB pectin (27%), which can be interpreted as due to the presence of metallic palladium in the nanocomposite.

The morphology and size of the nanocomposite were evaluated by SEM and TEM analysis. The SEM image (Fig. 3A) reveals a rough surface with spherical particles present in typical cluster shapes. The TEM image confirmed the successful synthesis of PdNPs in spherical particles distributed in the range of 1–25 nm with a mean size of 6–12 nm (Fig. 3B). The crystalline structure of metallic palladium can be clearly observed from the HRTEM image and SAED pattern (Fig. 3C). The HRTEM image displays the fringe lattice of the crystalline phase with a crystal spacing of 0.24 nm, which corresponds to the (111) plane of PdNPs. The SAED pattern showed bright circular rings related to the (111), (200), (220) and (311) Bragg's reflection planes of crystalline metallic palladium, which is in agreement with the earlier result of the XRD pattern. The scanning transmission electron microscopy (STEM) image (Fig. 3D) confirmed the presence of well-dispersed PdNPs embedded in the pectin without any agglomeration. EDX elemental mapping analysis (Fig. 3E–K) revealed PdNPs uniformly dispersed in the pectin chains relative to the C/O/Na/Ca elements of the framework. These results reflect good stability, a crystalline nanostructure and a high specific surface area, which are expected to aid effective catalysis for organic reactions.

2.3. Catalytic performance for the Heck coupling reaction

Heck coupling is an important C–C coupling reaction that is employed in many fields, such as the pharmaceutical industry, agriculture, and chemical engineering. In the present work, we applied the PdNPs@pectin catalyst for this coupling in water as a non-toxic solvent. The results are summarized in Table 1. It is well known that the Heck coupling reaction is strongly affected by the base agent and reaction time.[46] To explore these conditions, the reaction of styrene with iodobenzene was used as a model reaction. The investigation was carried out with three different alkalines, including K_3PO_4, CH_3COONa and Na_2CO_3 (entries 1–3). The results showed that the latter achieved a competitive yield of the product (76%) at 90 °C for 2 h. On the other hand, a significant yield of the product of up to 90% was achieved when the stirring was carried out within 6 h. The strong effect of the reaction time may be related to leaching of palladium into the aqueous solution and the diffusion rate of the reagents, which increase the accessibility of the active palladium sites.[47,48]

The best conditions were used to explore the applicability of the catalytic nanocomposite, and the influence of various substrates was investigated. Fluoride and methyl (CH_3) groups were utilized to study the effects of both reagents on the performance. Table 1 shows the successful conversion of iodobenzenes and vinylbenzenes into the respective products with good yields,

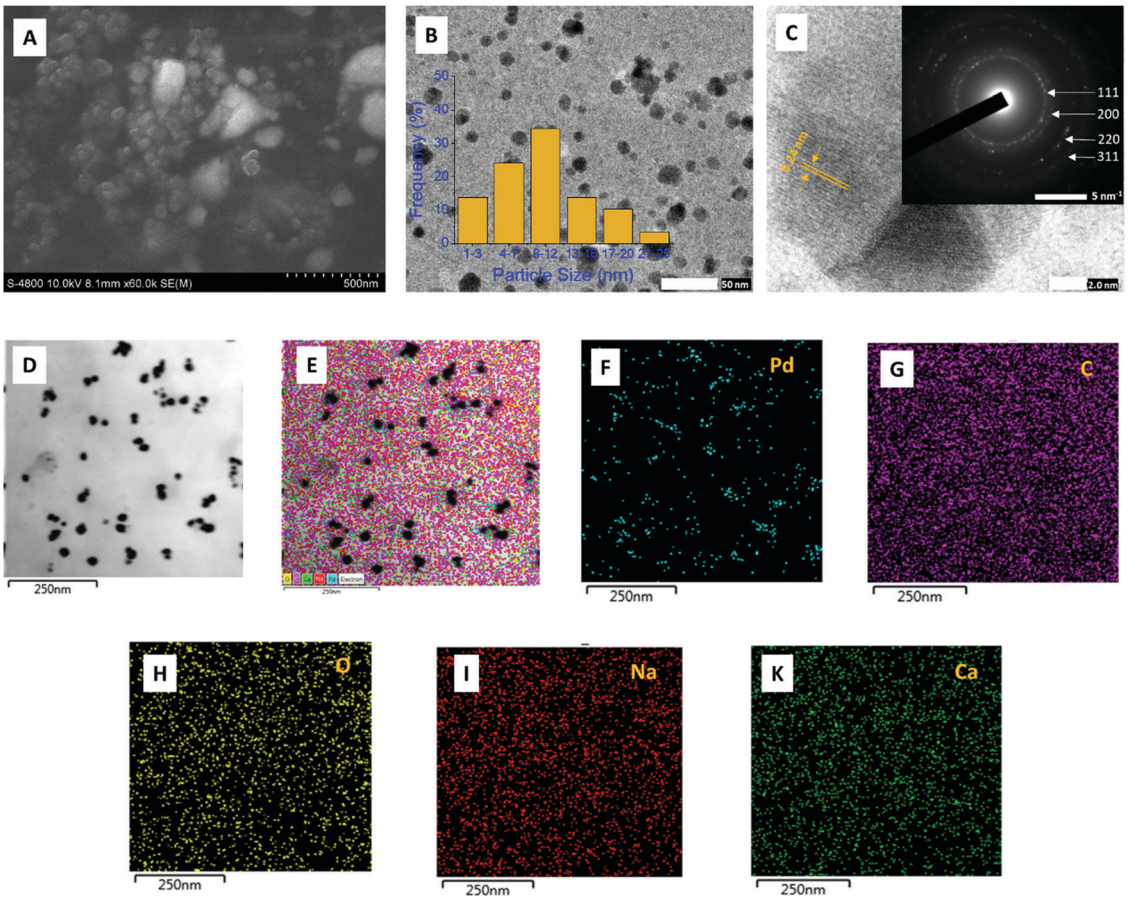

Fig. 3 SEM image (A), TEM image (B) and particle distribution (inset of B), HRTEM (C) and SAED patterns (inset of C), and STEM image (D) and EDX mapping (E–K) of PdNPs@pectin.

Table 1 Reaction conditions for Heck coupling in aqueous medium and catalysis of PdNPs@pectin

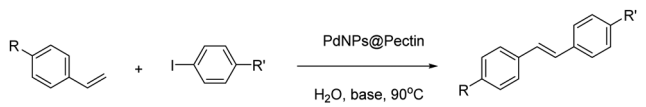

Entry	R	R′	Base	Time (h)	Isolated yield (%)
1	H	H	K_3PO_4	2	54
2	H	H	CH_3COONa	2	62
3	H	H	Na_2CO_3	2	76
4	H	H	Na_2CO_3	6	90
5	H	CH_3	Na_2CO_3	6	92
6	H	F	Na_2CO_3	6	89
7	CH_3	H	Na_2CO_3	6	86
8	CH_3	CH_3	Na_2CO_3	6	90
9	CH_3	F	Na_2CO_3	6	78
10	F	H	Na_2CO_3	6	90
11	F	CH_3	Na_2CO_3	6	87
12	F	F	Na_2CO_3	6	90

and PdNPs@pectin can be adapted to various substrates. The yields obtained are similar for both reagents using the different groups. For evaluation of the recycle capacity, the reaction mixture of iodobenzene and styrene was stirred in Na_2CO_3 for 6 h, and hexane was added to collect the product. The PdNPs catalyst was determined by a TEM image after the 6th run. The results are shown in Fig. 4. Isolated yields of about 87% were achieved after five recycles. The TEM image after the recycles confirmed the increase of the particle size, which indicated that the reaction occurred according to the Ostwald ripening process.[49] For the comparative study, the nanocomposite PdNPs@pectin catalyst possessed competitive catalytic activity in comparison with other catalyst systems for the Heck coupling reaction in water, as shown in Table S1 (ESI†). Therefore, the nanocomposite PdNPs@pectin is a promising material for the catalysis of C–C coupling.

2.4. Catalytic performance for reduction of nitrophenols

The catalytic reduction of nitrophenols possesses potential applications in pharmaceutical technology. It is well known that the products of the reduction of aminophenols are important intermediates for the synthesis of many drugs. Thus, it is particularly necessary to apply the simple and cost-efficient technique of this hydrogenation for pharmaceutical products. Additionally, reusability of the catalyst can significantly reduce the cost of the production technique. In this work, the reduction of *o*-, *m*-, and *p*-nitrophenol using $NaBH_4$ in water medium as a model reaction was used to evaluate the catalytic performance of PdNPs@pectin. The reaction without the catalyst is well known to be a thermodynamically favorable model; however, the kinetic

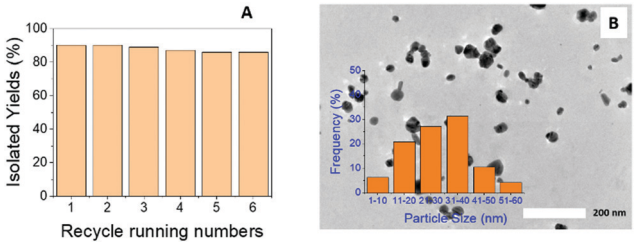

Fig. 4 Recyclable catalysis performance of PdNPs@pectin for Heck coupling between iodobenzene and styrene (A); TEM image and size distribution of the PdNPs after the 6th catalysis run (B).

barrier between BH_4^- and nitrophenolate ions results in a kinetically unfavorable reaction. This barrier can be overcome by using a metallic catalyst *via* an electron transfer mechanism in which borohydride and nitrophenolate ions can be absorbed and released on the surface of MNPs. Because a large excess of $NaBH_4$ (200 times) and a very small amount of the nanocomposite PdNPs@pectin (3 mg) were used, the kinetics of reduction should follow the pseudo first order reaction with respect to the nitrophenols.[50] For evaluation of the recyclability, the used nanocomposite was washed with distilled water and then ethanol before each reuse. The catalyst was tested for five reaction cycles.

The reduction of nitrophenols was directly monitored by using UV-vis measurements from a cuvette. The maximum peaks of the solutions containing *o*-, *m*- and *p*-nitrophenol in the presence of $NaBH_4$ were observed at 415 nm, 391 nm and 400 nm, respectively. When addition of the catalyst was completed, the decline of the absorbance values at the absorption peaks of the corresponding nitrophenolate ions and gradual increase of the peaks in the absorption range of 282–296 nm confirmed the conversion of the nitrophenols into the respective aminophenols. Fig. 5 showed that the reduction of *o*-, *m*- and *p*-nitrophenols was complete within 10 min, 6 min and 14 min,

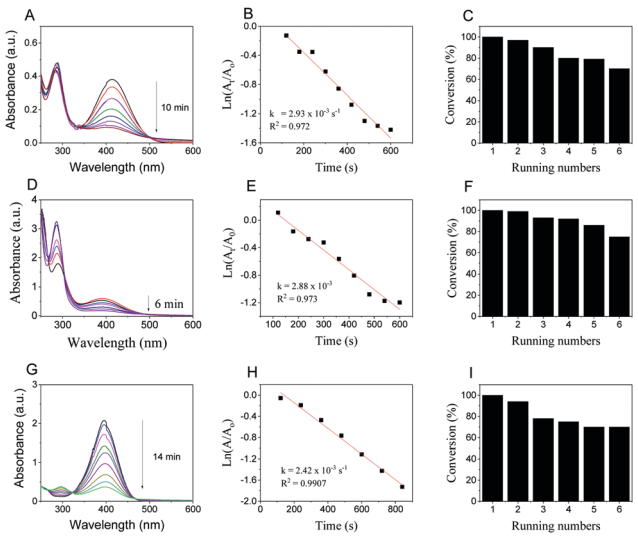

Fig. 5 UV-vis spectra (left), first order kinetics (middle) and conversion efficiencies for six running numbers (right) of *o*-nitrophenol (A–C), *m*-nitrophenol (D–F) and *p*-nitrophenol (G–I) in the presence of PdNPs@pectin.

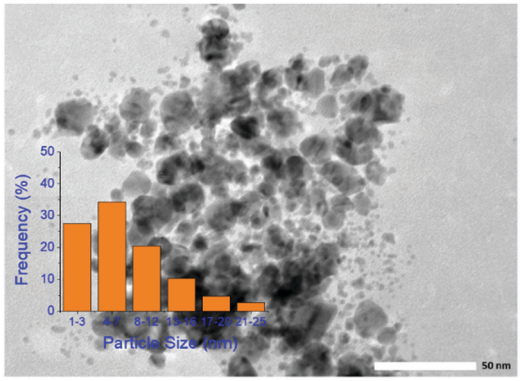

Fig. 6 TEM image and particle distribution (inset) of PdNPs@pectin used for reduction of *p*-nitrophenol after the 6th recycle run.

respectively. However, a different trend of the rate constants was observed in a decreasing order of *o*-nitrophenol (2.93×10^{-3} s^{-1}) > *m*-nitrophenol (2.88×10^{-3} s^{-1}) > *p*-nitrophenol (2.42×10^{-3} s^{-1}). These results showed that the catalytic performance of PdNPs@pectin is higher than that of other catalyst systems reported previously.[51–53] The recyclability of the nanocomposite is slightly different among nitrophenol substrates. Although a similar catalysis performance for all the nitrophenols was obtained at the 6th run (about 70%), a slow decline of the recycle performance was observed for the reduction of *o*- and *m*-nitrophenols, with above 90% at the 3th run, while the conversion of *p*-nitrophenol achieved only 75% for this run. The difference in the recycle performance may be due to the effect of the substrate structures on the adsorption or/and release processes on the catalyst surface. For further study, the TEM image of the catalyst after the 6th recycle run of *p*-nitrophenol was determined, as shown in Fig. 6. The results showed that the PdNPs existed in clusters, and the slightly smaller particle size may have been obtained because the product *p*-aminophenol stabilized the PdNPs after the catalysis process.[8] The decrease of the catalytic performance in the reduction of nitrophenols is attributed to the Pd clusters. Moreover, the loss of catalyst during the recycle process significantly affected the catalytic efficiency of PdNPs@pectin.[54] The PdNPs@pectin was shown to be a good recyclable catalyst in comparison with previous reports.[55,56]

2.5 Catalytic performance for the reduction of alkynes

The reduction of alkynes into *cis*-alkenes was performed using KOH in DMF solvent as a reductant, heated at 100 °C in the presence of PdNPs@pectin catalyst (2 mol%). The reaction was tested with different substrate structures. The results are summarized in Table 2. Excellent yields (above 90%) were obtained for the reduction of aromatic alkynes (entries 1–3), which confirmed that the catalytic performance was similar to that of $Pd(OAc)_2$ catalyst as previously reported.[35] Unfortunately, reduction of 3-butyn-1-ol (entry 4) and 3-hexyn-1-ol (entry 6) to the corresponding *cis*-alkenes was not observed, although the reaction time was lengthened to 12 h. However, the protection of these alcohols by tetrahydrofuran (OTHP) showed significant

Table 2 Reaction conditions for the Heck reaction in the presence of PdNPs@pectin

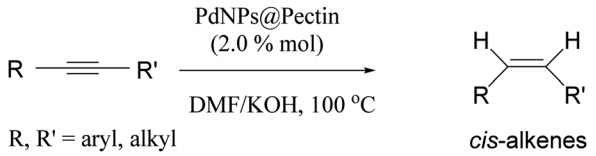

Entry	R	R′	Time (h)	Isolated yield (%)
1	H	C_6H_5	6	91
2	C_6H_5	C_6H_5	6	92
3	C_6H_5	*p*-$(CH_3)C_6H_5$	6	90
4	H–	$-CH_2CH_2OH$	12	Trace
5	H–	$-CH_2CH_2OTHP$	6	73
6	C_2H_5–	$-CH_2CH_2OH$	12	Trace
7	C_2H_5–	$-CH_2CH_2OTHP$	6	78

enhancements in the reaction yield. Isolated yields of the products of above 70% were obtained (entries 4 and 7). The lower performance in comparison with the reduction of aryl alkynes may be due to the high evaporation rate of alkyl alkenes. Moreover, the results indicated no influence of the triple bond position on the reduction of alkynes using PdNPs@pectin (entries 1, 2, 5 and 7). The ^{1}H-NMR data (entry 7, Supplementary data, ESI†) showed that the coupling constant between two protons of the double bond was estimated to be at 10.5–11.0 Hz, which confirmed the formation of *cis*-alkenes for the reduction of these alkynes.

2.6 Synthesis of insect pheromones

The reduction reaction of alkynes into *cis*-alkenes is a key step in the synthesis of many insect pheromones. In the present work, two pheromones of *P. xylostella* and *C. formicarius* which possessed *cis* configurations were selected to evaluate the application of the nanocomposite catalyst. *P. xylostella*, a cabbage moth, is a moth species of the family Plutellidae and is distributed worldwide. Its sex pheromone has been identified to have three components, including (*Z*)-11-hexadecen-1-ol, (*Z*)-11-hexadecenal and (*Z*)-11-hexadecen-1-yl acetate.[57–59] The composition for effective insect attraction is strongly dependent on the original insect; however, the acetate derivative is well known to be a major component of the sex pheromone.[60–62] Therefore, facile synthesis of (*Z*)-11-hexadecen-1-yl acetate is a particularly important key to apply this pheromone in field trials. The synthetic route of this component is presented in Scheme 1. A coupling between 1-hexynyllithium and 2-((10-bromodecanyl)oxy)tetrahydro-2*H*-pyran (**2**) was performed to obtain the derivative of hexadecyne (**3**). The reduction of (**3**) was carried out in the presence of PdNPs@pectin to afford (**4**) in a yield of 91%. The protective group cleavage was performed with PTSA, followed by acetylation with acetic anhydride in the presence of pyridine to obtain the pheromone (*Z*)-11-hexadecen-1-yl acetate (**5**) in a yield of 89% for two steps. A total yield for the synthesis of pheromone **5** of up to 70% was achieved. All pure compounds were identified by NMR spectra.

Cylas formicarius, a species of sweet potato weevil of the family Brentidae, is widely distributed worldwide. Its sex pheromone was identified as (*Z*)-3-dodecen-1-yl (*E*)-2-butenoate.[63] The synthetic route is described in Scheme 2. The key reactions used are similar to the synthesis of *P. xylostella* pheromone. The derivative of dodecyne (**8**) was obtained by a coupling reaction between a lithium reagent prepared from (**6**) and octyl bromide (**7**). The reduction of (**8**) was performed using KOH/DMF in the presence of PdNPs@pectin at 100 °C, followed by protective group cleavage to afford (*Z*)-3-dodecen-1-ol (**9**) in a yield of 90% for two steps. The esterification of compound (**9**) used (*E*)-2-butenoyl chloride in pyridine to obtain pheromone **10** in a yield of 86%. ^{1}H-NMR data of **9** and **10** showed a coupling constant of the two protons of double bond at about 10.5–11.0 Hz, which confirmed the *cis*-configuration of the synthesized alkene. The total yield achieved for the synthesis of pheromone **10** was about 68%.

3. Experimental

3.1. Materials

All chemicals were used as received without further purification. The major reagents, including vinylbenzenes, iodobenzenes, palladium acetate, nitrophenols, and sodium borohydride ($NaBH_4$), were purchased from Acros (Belgium). Diphenyl acetylenes were synthesized according to a previous report. *Cyclea barbata* was collected from Ho Chi Minh city. Deionized water was used throughout.

3.2. Preparation of *Cyclea barbata* pectin

Extract of *C. barbata* (CB) pectin was carried out according to a previous report with slight modification.[38] Briefly, dried *C. barbata* leaf powder (40 g) was ground well and stirred with water (500 mL) at room temperature. The extract was filtered rapidly under vacuum. Ethanol was added to the extract, and the precipitated pectin was separated from aqueous solution. The obtained pectin was centrifugated and washed with water (20 mL × 3). The pectin was freeze-fried for 24 h. The samples were stored at room temperature for further use.

3.3. Synthesis of PdNPs@pectin

The pectin (0.50 g) was stirred in water (50 mL) for 2 h. Then, 5 mL of $Pd(OAc)_2$ solution in DMSO (30.0 mg mL^{-1}) was dropped into a gel solution of the pectin. The yellow solution was stirred at 100 °C (1200 rpm) for 1 h to obtain a black solution, which confirmed the conversion of Pd^{2+} ions into PdNPs. PdNPs@pectin was separated and washed by a centrifugal process (3000 rpm, 30 °C, 30 min). The nanocomposite powder was dried at 60 °C for 12 h to obtain the composite PdNPs@pectin (0.32 g, 49.2%). The nanocomposite was stored at room temperature for further use.

3.4. Physicochemical characterization of PdNPs@pectin

UV-Vis spectroscopy was carried out on a JASCO V-630 spectrophotometer (U.S.A.) in the wavelength range of 200–700 nm. The Fourier-transform infrared (FTIR) spectra of the gum and PdNPs@pectin samples were measured on a FTIR spectrophotometer (Bruker, Tensor 27, Germany). The X-ray diffraction (XRD)

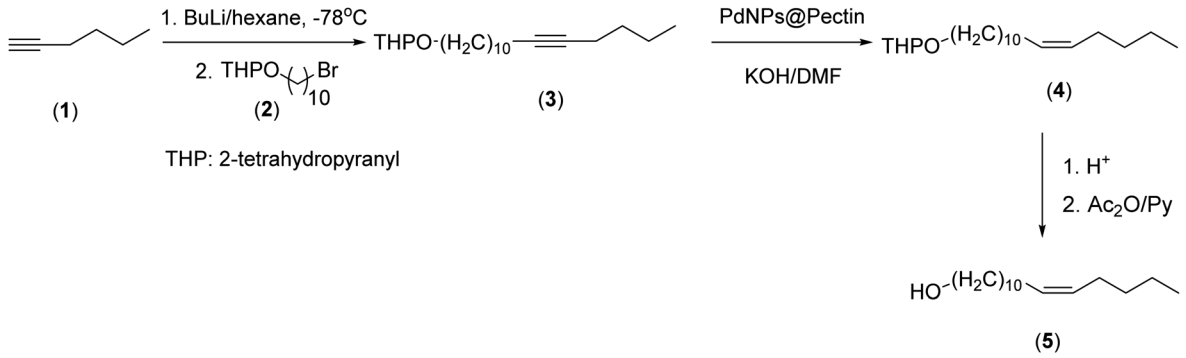

Scheme 1 Synthesis of *Plutella xylostella* pheromone.

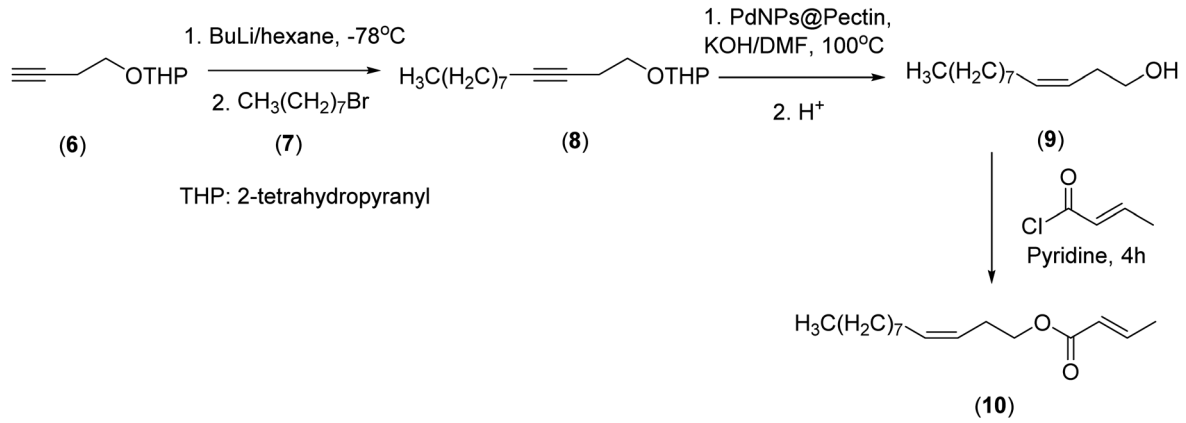

Scheme 2 Synthesis of *Cylas formicarius* pheromone.

pattern of PdNPs crystal was obtained on an X-ray diffractometer (Bruker, Model-D8 Advance). An aqueous solution of the nanocomposite was used to determine the particle size and zeta potential using a nanoPartica Horiba SZ-100 analyzer (Japan) at 25 °C. The morphology and crystalline structure of the nanocomposite were analyzed using field emission scanning electron microscopy (FESEM, JSM7401F, Japan) and high resolution transmission electron microscopy (HRTEM, JEOL JEM2100) – selected area electron diffraction (SAED). The chemical elements and elemental distribution in the nanocomposite were identified by an energy dispersive X-ray spectroscopy (EDX) analyzer (Horiba, EMAX ENERGY EX-400). Thermogravimetry (TG) analysis was performed on a LabSys evo S60/58988 Thermoanalyzer (Setaram, France) in the temperature range from 30 °C to 800 °C at a heating rate of 10 °C min^{-1} in air atmosphere. ^1H (500 MHz) and ^{13}C (125 MHz) NMR spectra were recorded on a NMR spectrometer (Bruker Advance 500) using $CDCl_3$ solvent and tetramethylsilane (TMS) as an internal standard. GC analyses were carried out using an Agilent Technologies 6890N chromatograph (USA) with an HP-5MS column.

3.5. Catalytic activity for Heck coupling

In a 25 mL round-bottom flask equipped with a magnetic stirrer and a reflux condenser, iodobenzenes (1.0 mmol), vinylbenzenes (1.1 mmol), bases (2 mmol) and PdNPs@pectin powder (6.4 mg, 0.7% mol) were added to 1 mL of water. The mixture was stirred at 100 °C. After cooling the solution, ethyl acetate (20 mL) was added. The water layer was separated and extracted. The organic layer was collected and washed with water. The solvent was evaporated under reduced pressure. The product was purified by silica gel column chromatography eluting with an ethyl acetate and hexane mixture. The purity of the product was determined by ^1H-NMR measurements. For the recycling, after completing the reaction, hexane was added to the reaction mixture and the product was collected from the organic layer. For the next reaction, the mixture of iodobenzene and styrene was added to the aqueous layer and stirred for 6 h.

3.6. Catalytic activity for reduction of nitrophenols

Catalytic reduction of *o*-, *m*-, *p*-nitrophenol in the presence of PdNPs@pectin was investigated at room temperature in aqueous medium, and an excess amount of $NaBH_4$ was used as a reductant. Each nitrophenol (2.5 mL, 0.1 mM) and $NaBH_4$ solution (0.5 mL, 0.1 M) were placed into a cuvette, and the catalyst (3 mg) was added to the reaction mixture. The performance of the catalyst was determined by UV-vis measurements. The reaction was confirmed by a gradual decrease of absorbance at the corresponding peaks of nitrophenol. Due to the great amount of $NaBH_4$ and very small amount of the catalyst used, the reaction rate was evaluated according to the pseudo-first-order reaction with respect to nitrophenol. Thus, the kinetics of the reduction reaction was described by the equation $\ln(A_t/A_0) = -kt$, where k is the reaction rate

constant (s^{-1}); t is the reaction time (s); and A_0 and A_t are the nitrophenol absorbances at the initial time and t, respectively. The rate constant could be found from the slope of the line generated by plots of $\ln(A_t/A_0)$ *versus* the reaction time. For evaluation of the reuse performance of the catalyst, PdNPs@pectin was separated and washed with water and then ethanol several times before reuse.

3.7. Catalytic activity for reduction of alkynes

Alkynes (0.25 mmol), KOH (30.7 mg), DMF (2.0 mL) and PdNPs (6.4 mg, 0.7% Pd catalyst) were added to a Pyrex screw-cap tube (25 mL) under nitrogen atmosphere. The mixture was stirred at 150 °C for 8 h. After the solution cooled, the mixture was diluted in ethyl acetate and water. The organic layer was separated and washed with water. The solvent was evaporated and the crude product was purified by silica gel column chromatography eluting with hexane/diethyl ether (9 : 1) or hexane/ethyl acetate (9 : 1).

3.8. Application of PdNPs@pectin catalyst for synthesis of insect pheromones

Synthesis of 2-(hexadec-11-yn-1-yloxy)tetrahydro-2*H*-pyran (3). A solution of 2.5 M *n*-BuLi in hexane (16.5 mL, 19.5 mmol) was introduced dropwise to a solution of 1-hexyne (**1**, 1.64 g, 20 mmol) in THF (10 mL), then stirred in N_2 atmosphere at −78 °C. The reaction mixture was warmed to room temperature and stirred for 1 hour. This reaction mixture was added to solid KI (0.25 g, 1.5 mmol) and 2-((10-bromodecyl)oxy)tetrahydro-2*H*-pyran (**2**, 4.82 g, 15 mmol) at room temperature. The resulting mixture was refluxed for 16 h. After cooling to room temperature, the reaction was quenched with saturated $NaHCO_3$ solution and the organic layer was separated. The aqueous layer was extracted with *n*-hexane. The combined organic layer was washed with brine, dried over $MgSO_4$, filtered, and concentrated *in vacuo*. The crude product was purified by column chromatography (silica gel, eluted by hexane to diethyl ether 9 : 1), affording **3** in 86% yield (4.15 g). ^{1}H NMR (500 MHz, $CDCl_3$, δ ppm): 4.57–4.58 (m, 1H), 3.70–3.89 (m, 2H), 3.36–3.52 (m, 2H), 2.12–2.16 (m, 4H), 1.52–1.84 (m, 8H), 1.28–1.48 (m, 18H), 0.89–0.92 (t, J = 7.5 Hz, 3H). ^{13}C NMR (125 MHz, $CDCl_3$, δ ppm): 98.9, 80.2, 80.2, 67.7, 62.3, 31.3, 29.8, 29.8, 29.6, 29.5, 29.2, 29.1, 28.9, 26.3, 25.5, 21.9, 19.7, 18.8, 18.5, 13.6.

Synthesis of (*Z*)-2-(hexadec-11-en-1-yloxy)tetrahydro-2*H*-pyran (4). To a mixture of alkyne **3** (0.55 g, 1.7 mmol), ground KOH powder (0.17 g, 2.55 mmol), and PdNPs@pectin (2% mol) in a thick-walled Pyrex seal tube was added degassed DMF (10 mL). The tube was sealed, and the reaction mixture was stirred vigorously at 145 °C for 6 hours. After cooling to room temperature, the cap was opened carefully and the resulting suspension was passed through a silica gel bed and washed with *n*-hexane. The combined filtrate was washed with water (50 ml × 5) to remove DMF. The organic layer was dried over $MgSO_4$, filtered, and concentrated *in vacuo.* The crude product was purified by column chromatography (silica gel, eluted by hexane to diethyl ether 9 : 1), affording **4** as a pale yellow oil in 91% yield (0.5 g). ^{1}H NMR (500 MHz, $CDCl_3$, δ ppm): 5.34–5.39 (m, 2H), 4.57–4.58 (m, 2H), 3.70–3.89 (m, 2H), 3.36–3.52 (m, 2H), 1.95–2.02 (m, 4H), 1.52–1.85 (m, 8H), 1.28–1.49 (m, 18H), 0.868–0.916 (m, 3H). ^{13}C NMR (125 MHz, $CDCl_3$, δ ppm): 129.9, 129.8, 67.7, 62.3, 32.6, 31.9, 31.8, 29.8, 29.5, 29.5, 29.4, 29.43, 29.3, 29.1, 27.2, 26.9, 25.5, 22.3, 19.5, 13.9.

Synthesis of (*Z*)-11-hexadecenyl acetate (5). A mixture of alkene **4** (0.4 g, 1.34 mmol) and PTSA (0.011 g, 0.067 mmol) in MeOH was stirred at room temperature for 16 h. After the evaporation of MeOH, the residue was treated with $NaHCO_3$ solution and extracted with *n*-hexane. The combined organic layer was washed with brine, dried over $MgSO_4$, filtered and concentrated *in vacuo* to afford (*Z*)-hexadec-11-en-1-ol as a brown oil. The crude product was used directly for the next reaction without further purification.

A mixture of (*Z*)-hexadec-11-en-1-ol, pyridine (0.11 g, 1.05 mmol) and anhydric acetic acid (0.083 g, 1.05 mmol) was stirred at 0 °C for 2 h and then warmed to room temperature. After 24 h, the residue was treated with HCl solution (10%) and extracted with diethyl ether (50 mL × 3). The combined organic layer was washed with saturated $CuSO_4$, $NaHCO_3$, water, and brine, dried over $MgSO_4$, filtered, and concentrated *in vacuo*. The crude product was purified by column chromatography (silica gel, eluted by hexane to diethyl ether 9 : 1), affording pheromone **5** as a pale yellow oil (0.19 g, 89%). ^{1}H NMR (500 MHz, $CDCl_3$, δ ppm): 5.34–5.39 (m, 2H), 4.04–4.06 (*t*, J = 7.5 Hz, 2H), 2.01–2.03 (m, 4H), 2.04 (s, 1H), 1.60–1.63 (m, 2H), 1.26–1.34 (m, 18H), 0.88–0.91 (t, J = 7.5 Hz, 3H). ^{13}C NMR (125 MHz, $CDCl_3$, δ ppm): 171.2, 129.9, 129.9, 64.7, 31.9, 29.8, 29.7, 29.5, 29.5, 29.3, 29.3, 28.6, 27.2, 26.9, 25.9, 22.4, 21.0, 13.9.

Synthesis of 2-(dodec-3-yn-1-yloxy)tetrahydro-2*H*-pyran (8). A solution of 2.5 M *n*-BuLi in hexane (16.5 mL, 19.5 mmol) was introduced dropwise to a solution of 2-(but-3-yn-1-yloxy)tetrahydro-2*H*-pyran (**6**, 3.08 g, 20 mmol) in THF (10 mL), stirred in N_2 atmosphere, at −78 °C. The reaction mixture was warmed to room temperature and stirred for 1 hour. To this reaction mixture was added solid KI (0.25 g, 1.5 mmol) and 1-bromooctane (**7**, 2.88 g, 15 mmol) at room temperature. The resulting mixture was refluxed for 16 h. After cooling to room temperature, the reaction was quenched with saturated $NaHCO_3$ solution and the organic layer was separated. The aqueous layer was extracted with *n*-hexane. The combined organic layer was washed with brine, dried over $MgSO_4$, filtered, and concentrated *in vacuo*. The crude product was purified by column chromatography (silica gel, eluted by hexane to diethyl ether 9 : 1), affording **8** (3.51 g, 88%). Bp. 150–153 °C/2 mmHg. ^{1}H NMR (500 MHz, $CDCl_3$, δ ppm): 4.64–4.65 (m, 1H), 3.76–3.91 (m, 2H), 3.48–3.55 (m, 2H), 2.43–2.47 (m, 2H), 2.11–2.15 (m, 2H), 1.27–1.85 (m, 18H), 0.88 (t, J = 7 Hz, 3H). ^{13}C NMR (125 MHz, $CDCl_3$, δ ppm): 98.7, 81.4, 76.7, 66.3, 62.2, 31.8, 30.6, 29.2, 29.1, 29.0, 28.9, 25.5, 22.6, 20.2, 19.4, 18.7, 14.1.

Synthesis of (*Z*)-dodec-3-en-1-ol (9). To a mixture of alkyne **8** (0.45 g, 1.7 mmol), ground KOH powder (0.17 g, 2.55 mmol), and PdNPs@pectin (2% mol) in a thick-walled Pyrex seal tube was added degassed DMF (10 mL). The tube was sealed, and the reaction mixture was stirred vigorously at 145 °C for 6 hours. After cooling to room temperature, the cap was opened carefully and the resulting suspension was passed through a silica gel bed and washed with *n*-hexane. The combined filtrate was

washed with water (50 ml × 5) to remove DMF. The organic layer was dried over $MgSO_4$, filtered, and concentrated *in vacuo.* The crude alkene product was used directly for the next reaction without further purification.

A mixture of crude alkene and PTSA (0.011 g, 0.067 mmol) in MeOH was stirred at room temperature for 16 h. After the evaporation of MeOH, the residue was treated with $NaHCO_3$ solution and extracted with *n*-hexane. The combined organic layer was washed with brine, dried over $MgSO_4$, filtered and concentrated *in vacuo*. The product was purified by column chromatography (silica gel, eluent of hexane to diethyl ether 4 : 1) to afford **9** (0.28 g, 90%). Bp: 120–125 °C/1 mmHg. ^{1}H NMR (500 MHz, $CDCl_3$, δ ppm): 5.53–5.58 (m, 1H), 5.33–5.39 (m, 1H), 3.62–3.65 (m, 2H), 2.32–2.35 (m, 2H), 2.04–2.08 (m, 2H), 1.27–1.54 (m, 13H), 0.88 (t, J = 7 Hz, 3H). ^{13}C NMR (125 MHz, $CDCl_3$, δ ppm): 133.6, 124.9, 62.4, 31.9, 30.8, 29.7, 29.5, 29.3, 29.3, 27.4, 22.7, 14.1.

Synthesis of (*Z*)-dodec-3-en-1-yl (*E*)-2-butenoate (10). A mixture of **9** (0.18 g, 1.0 mmol), pyridine (0.13 g, 1.25 mmol) and crotonoyl chloride (0.13 g, 1.25 mmol) was stirred at 0 °C for 2 h and then warmed to room temperature. After 24 h, the residue was treated with HCl solution (10%) and extracted with diethyl ether (50 mL × 3). The combined organic layer was washed with saturated $CuSO_4$, $NaHCO_3$, water, and brine, dried over $MgSO_4$, filtered, and concentrated *in vacuo*. The crude product was purified by column chromatography (silica gel, eluted by hexane to diethyl ether 9 : 2), affording pheromone **10** as a pale yellow oil (0.19 g, 86%). Bp: 104–106 °C/0.1 mmHg. ^{1}H NMR (500 MHz, $CDCl_3$, δ ppm): 6.93–7.00 (dq, J = 15.5 Hz, 7.0 Hz, 1H), 5.82–5.86 (dq, J = 15.5 Hz, 1.5 Hz, 1H), 5.48–5.53 (dtt, J = 11.0 Hz, 7.0 Hz, 1.5 Hz, 1H), 5.33–5.38 (dtt, J = 11.0 Hz, 7.5 Hz, 2.0 Hz), 4.12 (t, J = 7 Hz, 2H), 2.40 (q, J = 7.0 Hz, 2H), 1.87 (dd, J = 7 Hz, 1.5 Hz, 3H), 1.26–1.36 (m, 12H), 0.88 (t, J = 7 Hz, 3H). ^{13}C NMR (125 MHz, $CDCl_3$, δ ppm): 166.6, 144.5, 132.9, 124.4, 122.8, 63.7, 31.9, 29.7, 29.6, 29.5, 29.2, 27.3, 26.9, 22.7, 17.9, 14.1.

4. Conclusions

We investigated an effective method for *in situ* synthesis of PdNPs using *Cyclea barbata* pectin as a reduction and stabilization agent. The nanocomposite was well characterized by analysis techniques. The nanocomposite contained 30% palladium, and the average size of the nanoparticles was determined to be in the range of 6–12 nm. The catalytic activity of the nanocomposite was evaluated for the Heck coupling reaction, reduction of nitrophenols and reduction of alkynes. The high recyclable catalytic performance of Heck coupling in water medium was observed, and the Ostwald ripening mechanism of the PdNPs catalyst was confirmed. The recyclable catalytic reduction of *o*-, *m*- and *p*-nitrophenols showed high efficiency, with five successful recycles, and the values of the rate constants were found to be 2.93×10^{-3} s^{-1}, 2.88×10^{-3} s^{-1} and 2.42×10^{-3} s^{-1}, respectively. The recycle capacity of the nanocomposite was well recorded for five catalysis cycles. The effective reduction of alkynes into *cis*-alkenes was observed for both the aromatic and steric alkynes. This reaction was also utilized to straightforwardly synthesize two pheromones of *Plutella xylostella* and *Cylas formicarius* which possessed *cis*-configurations. Therefore, this catalyst reveals wide potential applications, such as in pharmaceutical, agricultural and environmental fields.

Conflicts of interest

No potential conflict of interest was reported by the authors.

Acknowledgements

The authors are thankful to Vietnam Academy of Science and Technology (VAST) for funding this project (NCVCC15.01/20-20).

Notes and references

1 A. Bej, K. Ghosh, A. Sarkar and D. W. Knight, *RSC Adv.*, 2016, **6**, 11446–11453.
2 F. W. Campbell and R. G. Compton, *Anal. Bioanal. Chem.*, 2010, **396**, 241–259.
3 I. Saldan, Y. Semenyuk, I. Marchuk and O. Reshetnyak, *J. Mater. Sci.*, 2015, **50**, 2337–2354.
4 A. M. Trzeciak and A. W. Augustyniak, *Coord. Chem. Rev.*, 2019, **384**, 1–20.
5 S. Luo, Z. Zeng, G. Zeng, Z. Liu, R. Xiao, M. Chen, L. Tang, W. Tang, C. Lai, M. Cheng, B. Shao, Q. Liang, H. Wang and D. Jiang, *ACS Appl. Mater. Interfaces*, 2019, **11**, 32579–32598.
6 F. Qazi, Z. Hussain and M. N. Tahir, *RSC Adv.*, 2016, **6**, 60277–60286.
7 F. Christoffel and T. R. Ward, *Catal. Lett.*, 2018, **148**, 489–511.
8 T.-D. Nguyen, T.-T. Vo, C.-H. Nguyen, V.-D. Doan and C.-H. Dang, *J. Mol. Liq.*, 2019, **276**, 927–935.
9 M. Martins, C. Mourato, S. Sanches, J. P. Noronha, M. T. B. Crespo and I. A. C. Pereira, *Water Res.*, 2017, **108**, 160–168.
10 C. P. Adams, K. A. Walker, S. O. Obare and K. M. Docherty, *PLoS One*, 2014, **9**, e85981.
11 D. Astruc, *Inorg. Chem.*, 2007, **46**, 1884–1894.
12 I. Favier, D. Pla and M. Gómez, *Chem. Rev.*, 2020, **120**, 1146–1183.
13 M. Pérez-Lorenzo, *J. Phys. Chem. Lett.*, 2012, **3**, 167–174.
14 R. Majumdar, S. Tantayanon and B. G. Bag, *Chem. – Asian J.*, 2016, **11**, 2406–2414.
15 R. Majumdar, S. Tantayanon and B. G. Bag, *Int. Nano Lett.*, 2017, 267–274.
16 P. P. Mpungose, Z. P. Vundla, G. E. M. Maguire and H. B. Friedric, *Molecules*, 2018, **23**, 1676.
17 L. Yu, Y. Huang, Z. Wei, Y. Ding, C. Su and Q. Xu, *J. Org. Chem.*, 2015, **80**, 8677–8683.
18 L. O. Nyangasi, D. M. Andala, C. O. Onindo, J. C. Ngila, B. C. E. Makhubela and E. M. Ngigi, *J. Nanomater.*, 2017, **2017**, 8290892.
19 R. Mangaiyarkarasi, M. Priyanga, N. Santhiya and S. Umadevi, *J. Mol. Liq.*, 2020, **310**, 113241.

20 G. Zhang, H. Zhou, J. Hu, M. Liu and Y. Kuang, *Green Chem.*, 2009, **11**, 1428–1432.
21 V. Calo, A. Nacci, A. Monopoli, A. Fornaro, L. Sabbatini, N. Cioffi and N. Ditaranto, *Organometallics*, 2004, **23**, 5154–5158.
22 A. I. Ayad, C. B. Marín, E. Colaco, C. Lefevre, C. Méthivier, A. O. Driss, J. Landoulsi and E. Guénin, *Green Chem.*, 2019, **21**, 6646–6657.
23 F. Diler, H. Burhan, H. Genc, E. Kuyuldar, M. Zengin, K. Cellat and F. Sen, *J. Mol. Liq.*, 2020, **298**, 111967.
24 R. Majumdar, B. G. Bag and P. Ghosh, *Appl. Nanosci.*, 2016, **6**, 521–528.
25 S. Furukawa and T. Komatsu, *ACS Catal.*, 2016, **6**, 2121–2125.
26 B. M. Trost, Z. T. Ball and T. Jöge, *J. Am. Chem. Soc.*, 2002, **124**, 7922–7923.
27 K. Chernichenko, Á. Madarász, I. Pápai, M. Nieger, M. Leskelä and T. Repo, *Nat. Chem.*, 2013, **5**, 718–723.
28 F. A. Westerhaus, R. V. Jagadeesh, G. Wienhöfer, M. M. Pohl, J. Radnik, A. E. Surkus, J. Rabeah, K. Junge, H. Junge, M. Nielsen, A. Brückner and M. Beller, *Nat. Chem.*, 2013, **5**, 537–543.
29 J. A. Delgado, O. Benkirane, C. Claver, D. Curulla-Ferré and C. Godard, *Dalton Trans.*, 2017, **46**, 12381–12403.
30 H. G. Bilgicli, H. Burhan, F. Diler, K. Cellat, E. Kuyuldar, M. Zengin and F. Sen, *Microporous Mesoporous Mater.*, 2020, **296**, 110014.
31 L. He, Y. Huang, A. Wang, X. Wang, X. Chen, J. J. Delgado and T. Zhang, *Angew. Chem., Int. Ed.*, 2012, **51**, 6191–6194.
32 R. Shen, T. Chen, Y. Zhao, R. Qiu, Y. Zhou, S. Yin, X. Wang, M. Goto and L. B. Han, *J. Am. Chem. Soc.*, 2011, **133**, 17037–17044.
33 K. Li, R. Khan, X. Zhang, Y. Gao, Y. Zhou, H. Tan, J. Chen and B. Fan, *Chem. Commun.*, 2019, **55**, 5663–5666.
34 Q. Ge, J. Ran, L. Wu and T. Xu, *J. Appl. Polym. Sci.*, 2015, **132**, 41268.
35 J. Li, R. Hua and T. Liu, *J. Org. Chem.*, 2010, **75**, 2966–2970.
36 S. Kusmardiyani, M. Insanu and M. A. Asyhar, *Procedia Chem.*, 2014, **13**, 194–197.
37 A. Arkarapanthu, V. Chavasit, P. Sungpuag and L. Phuphathanaphong, *J. Sci. Food Agric.*, 2005, **85**, 1741–1749.
38 O. Yuliarti and R. M. B. Othman, *Food Hydrocolloids*, 2018, **81**, 300–311.
39 W. Zhang, X. J. Zhao, Y. Jiang and Z. Zhou, *Inorg. Nano-Met. Chem.*, 2017, **47**, 15–20.
40 M. R. El-Aassar, O. M. Ibrahim, M. M. G. Fouda, N. G. El-Beheri and M. M. Agwa, *Carbohydr. Polym.*, 2020, **238**, 116175.
41 A. F. Fracasso, C. A. Perussello, D. Carpiné, C. L. D. O. Petkowicz and C. W. I. Haminiuk, *Int. J. Biol. Macromol.*, 2018, **109**, 784–792.
42 G. D. Manrique and F. M. Lajolo, *Postharvest Biol. Technol.*, 2002, **25**, 99–107.
43 K. Walbrück, F. Kuellmer, S. Witzleben and K. Guenther, *J. Nanomater.*, 2019, **2019**, 4758108.
44 A. JyothiKora and L. Rastogi, *Arabian J. Chem.*, 2018, **11**, 1097–1106.
45 A. Nuri, N. Vucetic, J. H. Smått, Y. Mansoori, J. P. Mikkola and D. Y. Murzin, *Catal. Lett.*, 2020, **150**, 2617–2629.
46 X. Pei, Y. Li, Y. Deng, L. Lu, W. Li, R. Shi, A. Lei and L. Zhang, *Carbohydr. Polym.*, 2021, **251**, 117020.
47 E. V. Vinogradova, C. Zhang, A. M. Spokoyny, B. L. Pentelute and S. L. Buchwald, *Nature*, 2015, **526**, 687–691.
48 R. Martínez, C. Carrillo-Carrión, P. Destito, A. Alvarez, M. Tomás-Gamasa, B. Pelaz, F. Lopez, J. L. Mascareñas and P. Pino, *Cell Rep. Phys. Sci.*, 2020, **1**, 100076.
49 R. Ouyang, J. X. Liu and W. X. Li, *J. Am. Chem. Soc.*, 2013, **135**(5), 1760–1771.
50 M. Kohantorabi and M. R. Gholami, *Ind. Eng. Chem. Res.*, 2017, **56**, 1159–1167.
51 T. D. Nguyen, C. H. Dang and D. T. Mai, *Carbohydr. Polym.*, 2018, **197**, 29–37.
52 Y. Zhao, H. Zhu, Q. Zhu, Y. Huang and Y. Xia, *J. Am. Chem. Soc.*, 2016, **138**, 16645–16654.
53 D. Berillo and A. Cundy, *Carbohydr. Polym.*, 2018, **192**, 166–175.
54 V. D. Doan, V. S. Luc, T. L. H. Nguyen, T. D. Nguyen and T. D. Nguyen, *Environ. Sci. Pollut. Res. Int.*, 2020, **27**, 6148–6162.
55 S. Hao, S. Li and Z. Jia, *J. Nanopart. Res.*, 2020, **22**, 270.
56 J. Li, X. Li, G. Han, C. Liu and X. Wang, *BioResources*, 2019, **14**, 3630–3650.
57 Y. S. Chow, S. C. Chiu and C. C. Chien, *Ann. Entomol. Soc. Am.*, 1974, **67**, 510–512.
58 Y. Tamaki, K. Kawasaki, H. Yamada, T. Koshihara, N. Osaki, T. Ando, S. Yoshida and H. Kankiohana, *Appl. Entomol. Zool.*, 1977, **12**, 208–210.
59 T. Koshihara and H. Yamada, *Jpn. J. Appl. Entomol. Zool.*, 1980, **24**, 6–12.
60 T. Ishii, K. Nakamura, K. Kawasaki, H. Nemoto, K. Takahashi and A. Kubota, *Jpn. J. Appl. Entomol. Zool.*, 1981, **25**, 71–76.
61 S. Lee, D. W. Lee and K. S. Boo, *J. Asia-Pac. Entomol.*, 2005, **8**, 243–248.
62 T. Jimena, P. Florencia, A. Silvana, S. Horacio, R. Adela and H. Viviana, *Agrociencia Uruguay*, 2016, **20**, 61–67.
63 R. R. Heath, J. A. Coffelt, P. E. Sonnet, F. I. Proshold, B. Dueben and J. H. Tumlinson, *J. Chem. Ecol.*, 1986, **12**, 489–1503.